Dd-STATb, a *Dictyostelium* STAT protein with a highly aberrant SH2 domain, functions as a regulator of gene expression during growth and early development

Natasha V. Zhukovskaya[1,*], Masashi Fukuzawa[1,*], Masatsune Tsujioka[1], Keith A. Jermyn[1], Takefumi Kawata[1], Tomoaki Abe[1], Marketa Zvelebil[2] and Jeffrey G. Williams[†]

[1]School of Life Sciences, University of Dundee, MSI/WTB Complex, Dow Street, Dundee DD1 5EH, UK
[2]University College London, Ludwig Institute for Cancer Research, The Cruciform Building, Gower Street, London WC1E 6BT, UK
*These authors contributed equally to this work
[†]Author for correspondence (e-mail: j.g.williams@dundee.ac.uk)

Accepted 16 October 2003

Development 131, 447-458
Published by The Company of Biologists 2004
doi:10.1242/dev.00927

Summary

***Dictyostelium*, the only known non-metazoan organism to employ SH2 domain:phosphotyrosine signaling, possesses STATs (signal transducers and activators of transcription) and protein kinases with orthodox SH2 domains. Here, however, we describe a novel *Dictyostelium* STAT containing a remarkably divergent SH2 domain. Dd-STATb displays a 15 amino acid insertion in its SH2 domain and the conserved and essential arginine residue, which interacts with phosphotyrosine in all other known SH2 domains, is substituted by leucine. Despite these abnormalities, Dd-STATb is biologically functional. It has a subtle role in growth, so that Dd-STATb-null cells are gradually lost from the population when they are co-cultured with parental cells, and microarray analysis identified several genes that are either underexpressed or overexpressed in the Dd-STATb null strain. The best characterised of these, discoidin 1, is a marker of the growth-development transition and it is overexpressed during growth and early development of Dd-STATb null cells. Dimerisation of STAT proteins occurs by mutual SH2 domain:phosphotyrosine interactions and dimerisation triggers STAT nuclear accumulation. Despite its aberrant SH2 domain, the Dd-STATb protein sediments at the size expected for a homodimer and it is constitutively enriched in the nucleus. Moreover, these properties are retained when the predicted site of tyrosine phosphorylation is substituted by phenylalanine. These observations suggest a non-canonical mode of activation of Dd-STATb that does not rely on orthodox SH2 domain:phosphotyrosine interactions.**

Supplemental data available online

Key words: *Dictyostelium*, STAT (signal transducer and activator of transcription) protein, SH2 domain:phosphotyrosine interaction, Growth control, Discoidin 1

Introduction

Interactions of SH2 domains with their phosphotyrosine-containing binding sites are integral to many signal transduction processes (reviewed by Pawson et al., 2001). An SH2 domain recognises a phosphotyrosine residue in the context of its flanking amino acid sequences and this imparts a degree of specificity to the interaction. Because the kinases that phosphorylate the tyrosine residue can be modulated in their activity, and because they display substrate specificity, SH2 domain-phosphotyrosine interactions afford a regulatable protein-protein interaction mechanism of great precision and flexibility.

The JAK-STAT signal transduction pathway is an example of 'fast track' signalling, from the plasma membrane to the nucleus, that relies upon SH2 domain-phosphotyrosine interactions (reviewed by Bromberg and Darnell, 2000; Chatterjee-Kishore et al., 2000; Horvath, 2000). When a cytokine binds to its receptor it induces multimerisation of the receptor chains and this activates a member of the JAK (Janus kinase) family, that tyrosine phosphorylates the receptor at specific positions. These tyrosine phosphorylated residues act as docking sites for the SH2 domains of STAT proteins and the STAT proteins are themselves tyrosine phosphorylated by the JAKs. The tyrosine phosphorylated STATs then undertake reciprocal SH2 domain-phosphotyrosine interactions and subsequently accumulate in the nucleus. Dimerisation has generally been thought to be dependent upon tyrosine phosphorylation (Shuai et al., 1994). However, in a recent study, unphosphorylated STAT1 and STAT3 molecules in unstimulated cells were shown to exist as homodimers (Braunstein et al., 2003). This suggests that tyrosine phosphorylation re-configures a pre-formed STAT dimer, such that it becomes biologically functional.

In *Dictyostelium* two STAT proteins and three SH2 domain-containing kinases have been described (Fukuzawa et al., 2001; Kawata et al., 1997; Moniakis et al., 2001). The Dd-STATa and Dd-STATc proteins contain, in their C-terminal proximal regions, an SH2 domain, a DNA-binding domain and a site of tyrosine phosphorylation. All three regions are conserved with respect to the metazoan STATs but the N-terminal-proximal regions of the two Dictyostelium STATs are highly diverged.

The Dd-STATa protein is activated by extracellular cAMP signalling and, at the slug stage of development, it becomes nuclear localised in the subset of pstA cells that constitute the slug tip (Araki et al., 1998). Dd-STATa functions there as an inducer of tip cell differentiation and a repressor of stalk cell differentiation (Fukuzawa and Williams, 2000; Mohanty et al., 1999). The Dd-STATc protein is activated by the stalk cell inducer DIF and, at the slug stage, Dd-STATc becomes nuclear localised in the pstO cells: a band of cells that lies immediately behind the pstA cells (Fukuzawa et al., 2001). Dd-STATc is a repressor that prevents pstA-specific gene expression in the pstO region (Fukuzawa et al., 2001).

During the hybridisation screen that yielded Dd-STATc (Fukuzawa et al., 2001) we isolated a third STAT: Dd-STATb. Here, we analyse Dd-STATb and show that, despite its highly unusual SH2 domain, it is a regulator of cell growth and of specific gene expression. We also analyse its biochemical properties and present evidence to suggest that it uses an unorthodox activation pathway.

Materials and methods

Cell culture, transformation and development

The Ax2 axenic derivative of NC4 (a gift of Dr G. Gerisch) was cultured at 22°C in HL5 medium (Watts and Ashworth, 1970) and transformed by electroporation. Transformants were selected at 10 μg/ml blasticidin S or at 10 μg/ml G418. Cells were developed either in shaken suspension in KK2 buffer (16.5 mM KH_2PO4, 3.8 mM K_2HPO_4, pH 6.2) at 2×10^7 cells/ml or, when late developmental stages were to be analysed, on 2% water agar plates.

Molecular modelling

A model of the Dd-STATb SH2 domain was built on the basis of the crystallographic structure of STAT1 (Chen et al., 1998). Initial alignment was made using the ClustalW method, this alignment was manually changed to take into account structural information from STAT1 and the Src SH2 domains. The final alignment was then used to construct the model by using the suite of programs within Quanta^{tm}. The target (Dd-STATb) protein and template (STAT1) were aligned by hand within Quanta^{tm}. Where the target sequence matched the template molecule, the residue coordinates from the template were transformed directly to the target. Where no equivalent atoms were found in the template molecule for the target protein, reference was made to a side chain rotamer library. This defines the most common conformation found for each side chain type (Summers and Karplus, 1989). Gaps in the target sequence were subjected to local energy minimisation to bring the core ends together and to alleviate local conformational strain. Although insertions in the target sequence were modelled by searching a fragment database of high-resolution structures (<1.5 Å) to find an appropriate template. The final structure was subjected to 500 steps of steepest gradient minimisation by the CHARMM program to make minor shifts in the coordinate positions, thereby alleviating steric clashes between atoms and obtaining a reasonable peptide geometry.

Creation of mutations in Dd-STATb

Dd-STATb cDNA fragments were cloned into the *Dictyostelium* vector pDXA and manipulated in *E. coli*. The Y to F mutation was created by PCR amplification using a mismatched primer, while the L to R mutation was created by site directed mutagenesis using the 'GeneEditor' kit (Promega, Ltd.). The mutated fragments, and the unmutated equivalent, were then cloned under the transcriptional control of the Actin 15 promoter and transformed into *Dictyostelium* using G418 selection.

Western transfer, immunoprecipitation and immunohistochemical staining

Western analysis was performed essentially as in Fukuzawa et al. (Fukuzawa et al., 2001) using 2×10^7 cells. The membrane was blocked with 5% milk powder then reacted overnight with the primary antibody C:STATb, a monoclonal antibody raised against the C-terminal 15 amino acids of Dd-STATb. It was used as a 1 in 20 dilution of the culture medium from C:STATb hybridoma cells. The majority of immunohistochemical analyses also used the C:STATb antibody but a few experiments employed a purified polyclonal antibody, pC:STATb. This was raised against the C-terminal 15 residue peptide that was used to raise C:STATb and affinity purified using the same peptide (Araki et al., 1998). Immunoprecipitation was performed using cell lysates prepared from growing cells again, as described by Araki et al. (Araki et al., 1998).

For immunochemical analysis, cells or developmental structures were fixed with 50% methanol/KK2 for 5 minutes, then with 100% methanol for 5 minutes. They were then stained with culture medium from the C:STATb hybridoma cells and detected using a goat anti-mouse secondary antibody labelled with Alexa Fluor 488 (Molecular Probes, Oregon, USA). The pC:STATb antibody was detected using a goat anti-rabbit secondary antibody labelled with Alexa Fluor 594 (Molecular Probes, Oregon, USA).

Generation of Dd-STATb null strains

The construct used to disrupt the Dd-STATb contains a genomic fragment with 1.4 kb of DNA upstream of the blasticidin resistance cassette and 0.55 kb downstream of the blasticidin resistance cassette. The blasticidin resistance cassette interrupts the Dd-STATb gene at its unique *Bam*HI site, at nucleotide 2536 within the coding region. The disruptant DNA fragment was excised with *Sal*I and *Hin*dIII and electroporated into *Dictyostelium*. This procedure gave a very high proportion (~90%) of homologous integrants.

Analysis of gene expression

Microarray analysis was performed using the PCR products from 1700 cDNA clones, chosen from a set of *Dictyostelium*-expressed sequence tags (Morio et al., 1998) (http://www.csm.biol.tsukuba.ac.jp/cDNAproject.html). The cDNA clones were amplified using primers flanking the vector sequences. The resultant PCR products were used as templates for a second PCR reaction, using nested primers, to generate probes. These DNA probes were then hybridised and analysed as described by Araki et al. (Araki et al., 2003) The images were analysed using GeneSpring (Silicin Genetics) and probes showing a twofold or greater enrichment (see text) were subjected to secondary analysis by northern transfer. This was performed as described elsewhere (Fukuzawa et al., 1997), using total RNA at 10 μg per lane but with 'ExpressHyb' solution (Clontech, Palo Alto, USA) used as the hybridisation buffer.

Sedimentation analysis of Dd-STATb

Extracts from cells growing at 2×10^6/ml were layered on 10%-40% glycerol gradient and centrifuged for 40 hours at 285,000 ***g*** in a Beckman SW41 rotor (Shuai et al., 1994).

Results

Dd-STATb has a highly unusual SH2 domain

The Dd-STATb cDNA was isolated by low stringency hybridisation using the SH2 domain of Dd-STATa as a probe (Fukuzawa et al., 2001). The C-terminal halves of the three Dictyostelium STAT proteins are devoid of CAA repeats and show strong mutual homology in their presumptive DNA binding domains, SH2 domains and sites of tyrosine phosphorylation (Fig. 1A). As in Dd-STATa and Dd-STATc,

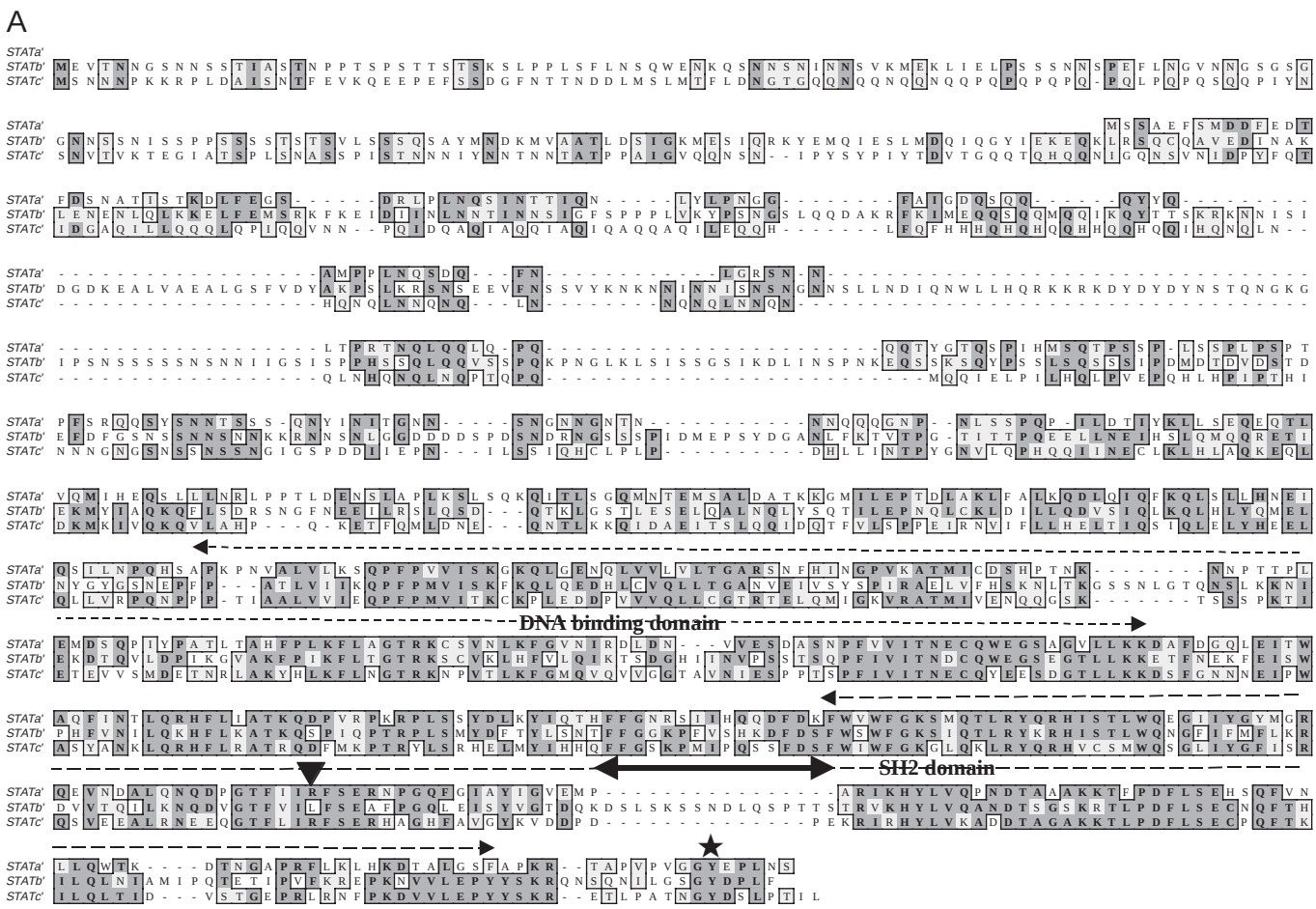

Fig. 1. Alignment of the Dd-STATa, b and c sequences after removal of their simple sequence component. The Accession Number of the complete predicted sequence of Dd-STATb is AJ581661 but here a truncated form of the sequence is presented. The N-terminal halves of Dd-STATa, b and c contain tracts of glutamine, asparagines and threonine. These are encoded by CAA repeats, a feature common to many *Dictyostelium* genes. In this alignment, Q, N and T tracts equal to or longer than three residues were omitted, to give Dd-STATa′ (633 of 707 residues), Dd-STATb′ (978 of 1147 residues)and Dd-STATc′ (819 of 929 residues). The three STATs display only scattered regions of short homology in their N-terminal-proximal regions. No functions have thus far been mapped to the N-terminal-proximal regions of Dd-STATa or Dd-STATc and a BLAST search using the N-terminal-proximal region of Dd-STATb also yielded no hits (the search was run at NCBI with amino acids 1 to 505 and using blastP with an ‘E’ value of 10). The predicted approximate positions of the DNA binding domains (closely spaced broken line), the SH2 domains (widely spaced broken line) and the site of the insertion in the Dd-STATb sequence (broad unbroken line) are indicated by double-headed arrows. The positions of the arginine to leucine substitution is indicated by a triangle, and the predicted site of tyrosine phosphorylation is indicated by an asterisk. (B) Alignment between the SH2 domains of Dd-STATs a to c, human STATs 1 to 6 and Src. The alignment was generated using ClustalW and then modified by hand to align the known secondary structure elements from STAT1 and the Src SH2 domain. This alignment was used in modelling the Dd-STATb SH2 domain (STATc). The dominant inserts are highlighted in yellow; red indicates identical residues; grey indicates similar residues. The inset shows a phylogenetic tree generated using the Nearest Neighbour joining method; blue boxes indicate proteins where a crystal structure is known.

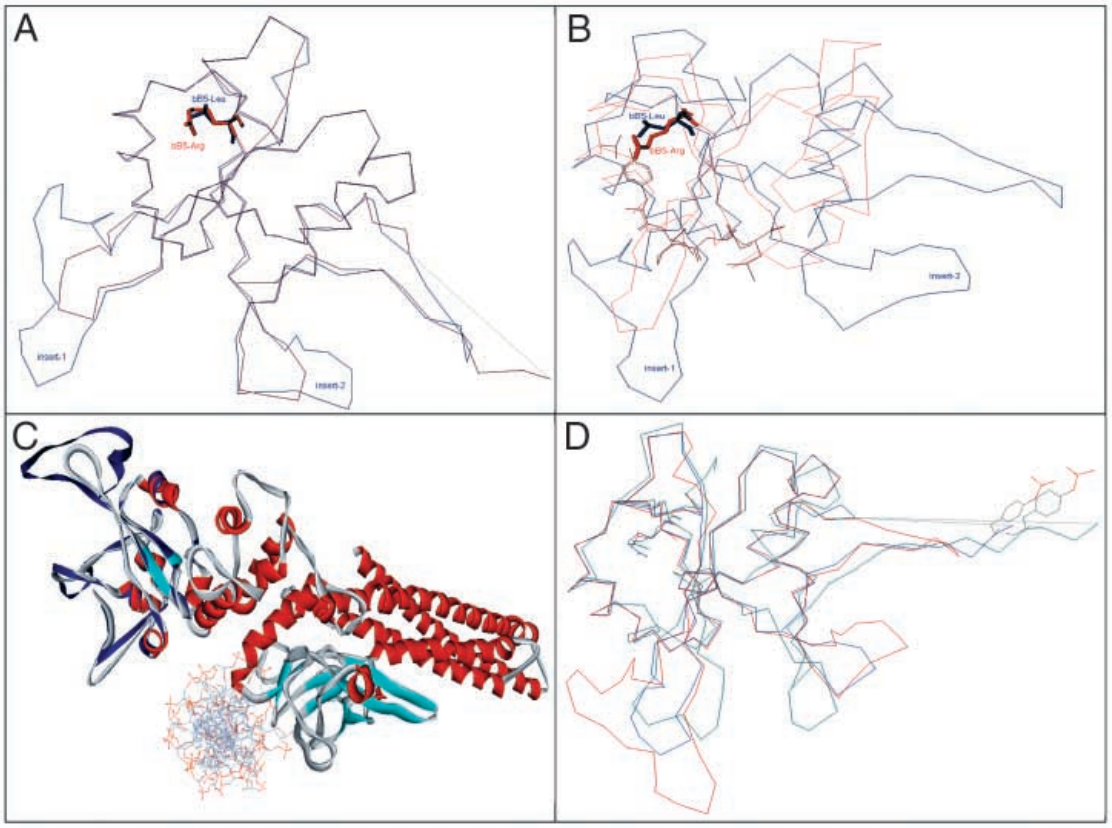

Fig. 2. Structural analysis of Dd-STATb. (A) The Cα trace of Dd-STATb (blue), superimposed on STAT1 (magenta), was used as a template for modelling Dd-STATb. The invariant arginine at position βB5 is shown in red (in STAT1) and its equivalent residue in Dd-STATb, a leucine, is shown in blue. The two main inserts are highlighted. (B) Dd-STATb is superimposed on the Src SH2 domain, with the arginine/leucine variation highlighted and the Src phosphopeptide also shown. (C) A ribbon diagram of Dd-STATb (in blue) superimposed on the whole structure of STAT1, showing that the position of the large insert (insert1) would not disrupt a similar dimerisation as that seen for STAT1. (D) The Cα trace for Dd-STATb (red), STAT1 (blue) and STAT3 (green). The phosphorylated Serine residues are shown in STAT1 and STAT3. It is apparent that the positions of insert 1 and insert 2 are regions of dissimilarity in both STAT1 and STAT3.

the predicted site of tyrosine phosphorylation of Dd-STATb (marked with an asterisk in Fig. 1A) is located very close to the C terminus.

The unique feature of Dd-STATb is its SH2 domain. Fig. 1B is an alignment between the SH2 domains of human STATs 1 to 6, Dd-STATs a to c and v-Src. In Dd-STATb, the invariant arginine residue (βB5 in standard SH2 domain numbering), that forms a bidentate ionic interaction with the tyrosine phosphate in all characterised SH2 domains, is replaced by a leucine residue (Fig. 1B and indicated with a triangle in Fig. 1A). In addition, there is a 15 amino acid insertion in the loop between β strands C and D (indicated with a double headed arrow in Fig. 1A and highlighted in yellow in 1B). This is in marked contrast to Dd-STATa and Dd-STATc, both of which conform well to the consensus sequence for STAT SH2 domains (Fukuzawa et al., 2001; Kawata et al., 1997). Fig. 1B also shows a phylogenetic tree for the above sequences. As might be expected, given the evolutionary separation involved, the three Dictyostelium STATs are more closely related to each other than to any one of the human STATs.

To further analyse the Dd-STATb SH2 domain peculiarities, a model based on the crystallographic structure of STAT1 (Chen et al., 1998) was built. The model illustrates the effects of the arginine to leucine change in more detail. Fig. 2A shows the Cα of Dd-STATb and the Cα of STAT1 superimposed, with the arginine and leucine residues highlighted. The large insertion (insert-1) is also obvious. The model identifies another shorter, region of insertion (insert 2), which was not as apparent from sequence alignment alone. The superposition of the Src-SH2 domain and its bound phosphopeptide with Dd-STATb shows that the βB5-leucine residue probably has little or no interaction with the tyrosine phosphate (Fig. 2B). However, arginine12 (which is either a lysine or arginine in the other SH2 domain sequences, Fig. 1B) is still able to form interactions with phosphotyrosine. The model (Fig. 2C) shows that the large insertion (insert 1) is predicted to have little or no effect on dimerisation or DNA binding. It may also be relevant that the regions of the two insertions are highly variable between STAT1 and STAT3 (Fig. 2D).

Dd-STATb is enriched in the nuclei of all cells during growth and development

A monoclonal antibody, the C:STATb antibody, was raised against a peptide with the sequence of the C-terminal 15 amino acids of Dd-STATb. When the C:STATb antibody is used to

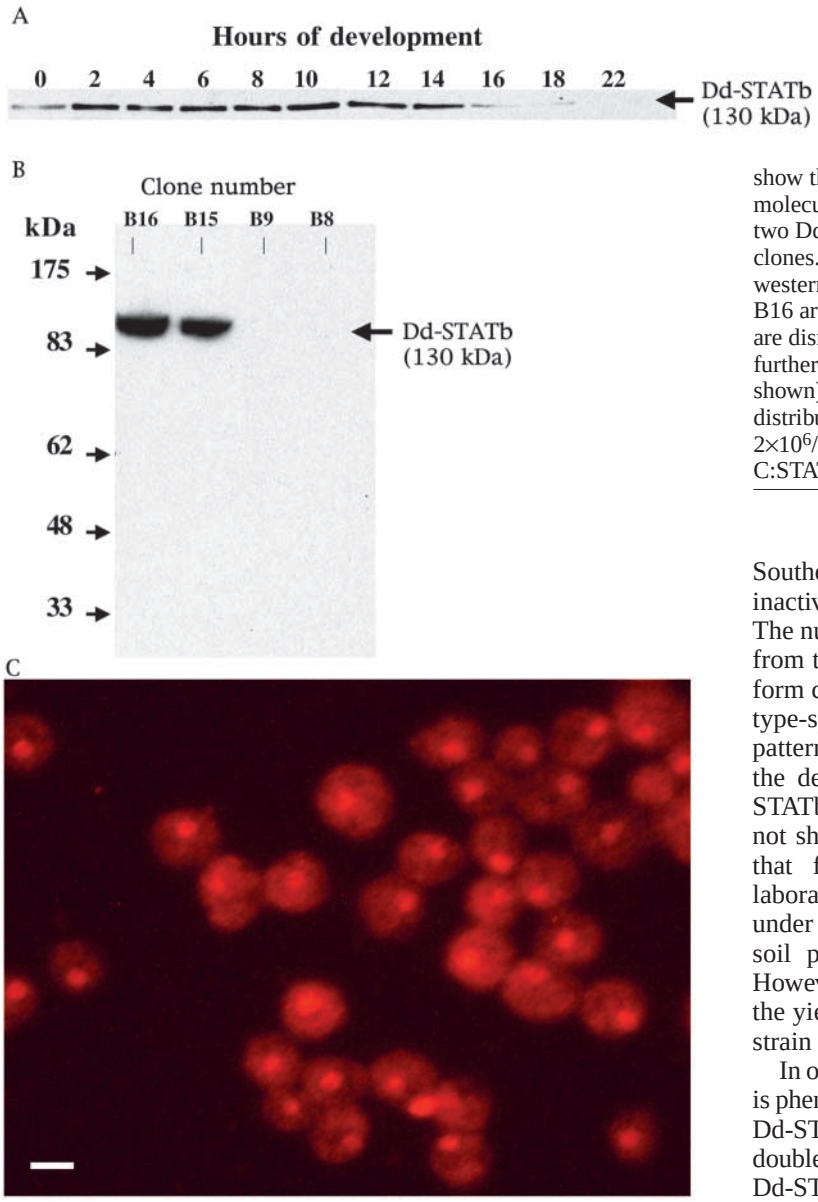

Fig. 3. (A) Western transfer analysis of Dd-STATb. Cells were allowed to develop on water agar, aliquots were harvested at the indicated times and they were subjected to western transfer analysis using the C:STATb antibody. This result, combined with other gel analyses using high molecular weight markers (B), show that Dd-STATb migrates with the expected approximate molecular weight of 130 kDa. (B) Western transfer analysis of two Dd-STATb disruptant clones and two random integrant clones. The four clones were grown to 2×10^6/ml and subjected to western transfer using the C:STATb antibody. Clones B15 and B16 are random integrant (Dd-STATb+) clones and B8 and B9 are disruptant (Dd-STATb–) clones. These assignments were further confirmed by immunohistochemical staining (data not shown). (C) Immunohistochemical analysis of the intracellular distribution of Dd-STATb in growing cells. Cells growing at 2×10^6/ml in HL5 medium were fixed and stained with the C:STATb antibody. Scale bar: 10 μm.

probe a Western blot of cell extracts, during both growth and early development, it detects a single protein of approximately 130 kDa, the predicted size of Dd-STATb (Fig. 3A). The 130 kDa protein is absent from Dd-STATb null strains (Fig. 3B). Later, during culmination, the apparent concentration of Dd-STATb falls (Fig. 3A). Immunohistochemical analysis shows that Dd-STATb is enriched in the nuclei of growing cells (Fig. 3C). Multicellular development was examined using wholemounts that were fixed and stained at different stages up to mid-culmination. Dd-STATb was enriched in the nuclei of all cells at all stages analysed (data not shown).

Generation and characterisation of a Dd-STATb null mutant and of double mutants with Dd-STATa and Dd-STATc

Dd-STATb null (Dd-STATb–) strains were generated by homologous recombination using a blasticidin-based gene disruption construct. Gene disruption was demonstrated, by Southern transfer (data not shown), and functional inactivation was confirmed by western transfer (Fig. 3B). The null strains grow with doubling times indistinguishable from the parental strain and develop, at a normal speed, to form correctly proportioned fruiting bodies. Moreover, cell type-specific reporter constructs all display normal staining patterns in Dd-STATb– strains (data not shown). We tested the detergent resistance of spores of wild type and Dd-STATb– strains and found them to be equally resistant (data not shown). A number of different gene disruptant strains that fail to show a developmental phenotype under laboratory conditions display a phenotype when developed under the more rigorous and natural conditions afforded by soil particles (Ponte et al., 1998; Ponte et al., 2000). However, when the Dd-STATb– strain is developed on soil, the yield of viable spores is just as high as for the parental strain (data not shown).

In order to determine whether the Dd-STATb null mutation is phenotypically silent because of mutually redundancy with Dd-STATa or Dd-STATc, we determined the phenotypes of double mutants of Dd-STATb with the other two STATs. A Dd-STATa–/Dd-STATb– double mutant shows the same developmental behaviour as a Dd-STATa– strain and a Dd-STATc–/Dd-STATb– strain is indistinguishable from a Dd-STATc– strain (data not shown). Thus, Dd-STATb does not appear to be functionally redundant with the other two known *Dictyostelium* STATs. One important caveat must, however, be applied in the case of Dd-STATa. Dd-STATa null cells arrest development early in culmination. Hence, redundancy between Dd-STATb and Dd-STATa in later development is intrinsically non-assayable.

Absence of the Dd-STATb protein places cells at a growth disadvantage

Despite our inability to detect any defect in the growth or development of Dd-STATb– cells, we reasoned that Dd-STATb must have a function that gives wild-type strains a selective advantage. Otherwise, its retention over evolutionary time would be very difficult to explain. We therefore performed growth competition experiments, in which mixtures of Dd-STATb– and Dd-STATb+ cells were repeatedly transferred to fresh medium after growth to saturation. The fractional

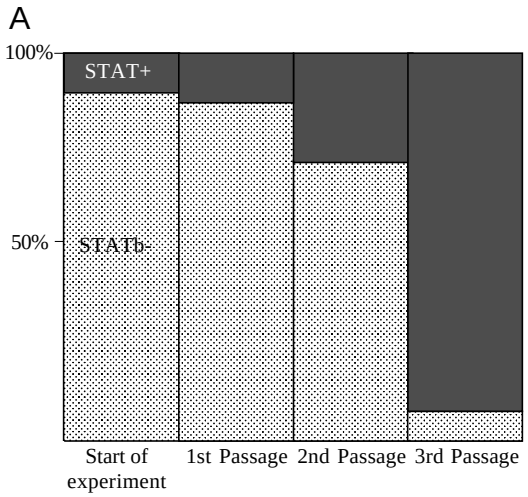

B

Pool 1	94% B-	3 passes →	10% B-
Pool 2	81% B-	4 passes →	14% B-
Pool 3	92% B-	5 passes →	25% B-
Pool 4	78% B-	4 passes →	33% B-
Pool 5	75% B-	4 passes →	10% B-
Average	84% B-	4 passes →	18%B-

Fig. 4. (A) Determination of the relative growth rates of Dd-STATb– and Dd-STATb+ cells. A co-cultivation experiment, with three cycles, was performed using a mixture of Dd-STATb– and Dd-STATb+ cells that were derived from a single transformation with the Dd-STATb disruption construct (see text). The cells were allowed to grow to saturation (~2×10^7/ml) and then diluted 1 in 100 for re-growth. (B) A compilation of five co-cultivation experiments. The first (top) experiment is that described in A and the other four experiments were performed in the same way. Although the rate of loss of the null cells was variable, the outcome was reproducible; the random integrant cells always came to dominate the population.

representation of Dd-STATb+ cells was determined at the end of each cycle of growth by immunostaining.

Initial experiments showed that the assay is extremely sensitive to intrinsic variations in the growth rate of the control, 'parental' strain. Hence, the experimental design we eventually adopted was to analyse entire pools of blasticidin resistant colonies, generated using the Dd-STATb disruption construct. Each pool derived from a separate transformation and contained the progeny of approximately 100-200 'founder' clones. The Dd-STATb disruption construct is very efficient and, at the start of each experiment, 80% to 90% of the cells contained a disrupted Dd-STATb gene. The remaining 10%-20% were cells where Dd-STATb was expressed normally and where the blasticidin resistance gene had presumably integrated, non-homologously, at random sites in the genome ('random integrants'). We reasoned that, if large numbers of cells were analysed (to average out the occasional effects that random integration of the vector might have on cell growth in particular clones), the random integrants would provide the best available 'isogenic' controls.

The results presented in Fig 4A are from a typical serial passage experiment and Fig. 4B is a summary of the results of four additional experiments. The proportion of Dd-STATb+ cells rose from ~15% to just over 80% during the course of four cycles of growth to saturation. Thus, Dd-STATb null cells are at a selective growth disadvantage as compared with control cells. It must, however, be stressed that this is a very subtle growth defect that is only revealed when Dd-STATb– cells are placed in competition with Dd-STATb+ cells, by growth through repeated cycles; parallel comparisons of the growth rates of separate Dd-STATb+ and Dd-STATb– cell populations, over just one growth cycle, are simply not sensitive enough to detect the difference.

In the above experiments, cells were grown to saturation. Hence, it seemed possible that Dd-STATb might be important in maintaining cell viability under starvation conditions, rather than in optimising the rate of growth. We therefore repeated the experiments, using a protocol whereby the cells were kept in exponential phase over multiple cycles of dilution and re-growth. This yielded very similar results, the fraction of Dd-STATb– cells decreased during serial passages (data not shown). Thus, Dd-STATb is essential for an optimal rate of cell growth rather than for cell survival under adverse conditions.

Micro-array analysis reveals gene expression changes in Dd-STATb null cells

The growth stage function of Dd-STATb, implied by the above competition studies, was analysed further using a microarray bearing PCR products from 1700 ESTs (Morio et al., 1998). The microarray was hybridised with equal amounts of parental and Dd-STATb– cell cDNAs, prepared using RNA from cells growing axenically. Thirty-eight ESTs showed hybridisation signals that differed at least twofold, between the Dd-STATb null strain and the random integrant, and that duplicated when the direction of dye labeling was reversed (Table 1).

For 29 of the ESTs, there was a higher level of hybridisation with the probe from Dd-STATb null cells, while another nine ESTs showed the converse behaviour. Northern transfer was used to confirm two of the microarray results (for smlA, discoidin 1). We also analysed two ESTs (HGPRT and DdCAD-1) that did not duplicate in the dye swap, using the criteria described above, but where the differential signal was convincing for just one of the labeling directions.

The northern transfer was performed, using RNA prepared from cells at different stages during growth to saturation. As expected, Dd-STATb– cells show a lower than normal level of expression of HGPRT and a higher than normal level of expression of smlA, discoidin 1 and DdCAD-1 (Fig. 5A). Because the level of discoidin 1 overexpression is relatively small, and only becomes manifest at low cell densities, we also compared discoidin 1 expression levels in five separate disruptant clones and five separate random integrant clones. All the Dd-STATb– strains display a several fold higher level of discoidin 1 expression than the random integrants (Fig. 5B).

Discoidin 1 displays two peaks of expression, one during the

Table 1. A list of the ESTs that display altered expression in Dd-STATb null cells

EST ID[†]	b+/b– (F)[‡]	b+/b– (R)[‡]	Comment
ESTs overexpressed in Dd-STATb null cells			
SSK554	2.65	3.0	No significant homology
SSK452	5.25	57.25	No significant homology
SSL314	3.89	2.27	No significant homology
SSL296	2.68	2.34	No significant homology
SSK649	2.24	3.58	Similar *Dictyostelium* CIGB
SSK726	18.58	3.10	No significant homology
SSJ635	5.17	2.09	Faint homology Arabidopsis RPP5 pn.
SSK241	2.29	3.56	Faint homology Drosophila RCG6432 pn
SSJ826	3.83	2.48	Similar to Mus tenascin-X protein
SSJ314	2.46	2.16	Faint homology Nematode F47A4.2 pn
SSM242	6.47	2.54	No significant homology
SSM776	11.79	15.78	Possible Ca-binding protein
SSM768	3.92	4.56	No significant homology
SSM146	3.01	6.35	Similar to Plasmodiumhypothetical pn.
SSL481	2.54	2.66	No significant homology
SSL591	2.06	2.85	Faint homology Methanobacterium pn
SSL427	2.94	2.06	No significant homology
SSL850	49.8	7.23	Dictyostelium discoidin 1c
SSH433	2.73	2.02	No significant homology
SSH823	2.66	2.02	Faint homology Acetyl-CoA transferrase
SSH209	3.79	4.73	No significant homology
SSH194	2.36	2.18	No significant homology
SSH238	7.41	4.54	Similar to Plasmodium hypothetical pn.
SSH132	4.44	2.08	Faint homology Methanococcus L23P pn
SSI313	2.73	2.17	No significant homology
SSI152	2.94	2.77	No significant homology
SSI438	8.75	22.9	No significant homology
SSI515	5.96	3.23	Dictyostelium SmlA protein
ESTs under-expressed in Dd-STATb null cells			
SSL550	0.01*	0.477	No significant homology
SSM419	0.01*	0.185	Faint homology to C. elegans ZC53.4 protein
SSM343	0.01*	0.329	Faint homology to D. melanogaster CG11931 protein
SSM781	0.01*	0.01*	No significant homology
SSM757	0.01*	0.398	Weak homology to B. mori cytochrome P450 .
SSH512	0.476	0.419	Weak homology to A. thaliana mitochondrial PSST subunit
SSH408	0.01*	0.488	No significant homology
SSJ456	0.01*	0.01*	Weak homology to histidine ammonia lyase
SSJ244	0.01*	0.01*	No significant homology

*Expressed as 0.01 becausee the apparent expression level in the null cells was less than zero.

[†]A list of all the ESTs used in the study is available as supplementary data.

[‡]The results for each EST are presented as the ratio of the signal in the random integrant to the signal in the gskA null strain (b+/b–) and are for each of the two directions in the dye swap: b+/b– (F) was cy3/cy5 and b+/b– (R) was cy5/cy3.

late log phase of growth the second during early development (Devine et al., 1982). We therefore compared the levels of discoidin 1 mRNA during development, using two random integrant clones and two Dd-STATb disruptant clones. The level of discoidin 1 expression at the peak of expression, i.e. at about 4 hours of development, is again several-fold higher in the two Dd-STATb– strains (Fig. 6).

Dd-STATb is present as an apparent dimer and does not appear to form a heterodimer with either Dd-STATa or Dd-STATc

Having shown that Dd-STATb regulates gene expression, we next investigated its biochemical functioning. When they are tyrosine phosphorylated, STAT proteins homo- or heterodimerise with other STATs, migrate to the nucleus and bind to DNA. This biological activation process is dependent upon SH2 domain:phosphotyrosine interactions (Shuai et al., 1994). Hence, it is important to know whether Dd-STATb protein, isolated from *Dictyostelium* cells, forms part of a dimer. This was assayed using glycerol gradients to estimate the size of the native protein.

When cells are exposed to a hyper-osmotic shock, Dd-STATc is activated and sediments on a glycerol gradient with the apparent molecular weight of a dimer (Fukuzawa et al., 2001; Araki et al., 2003). This provides a convenient size marker; because a Dd-STATc dimer has a predicted molecular weight of 214 kDa, whereas a Dd-STATb dimer has a predicted molecular weight of 260 kDa. Hence, gradient analysis of Dd-STATb was performed, using samples isolated from cells stimulated with sorbitol.

The glycerol gradient fractions were subjected to sequential western blot analysis, using antibodies directed against Dd-STATc and Dd-STATb. The sorbitol induction in this experiment was very efficient and most of the Dd-STATc protein sedimented as a dimer (Fig. 7). The Dd-STATb protein also sedimented in this region of the gradient; the DdSTATc peak is in fraction 11, whereas the DdSTATb protein sediments slightly more quickly and its peak lies between fractions 11

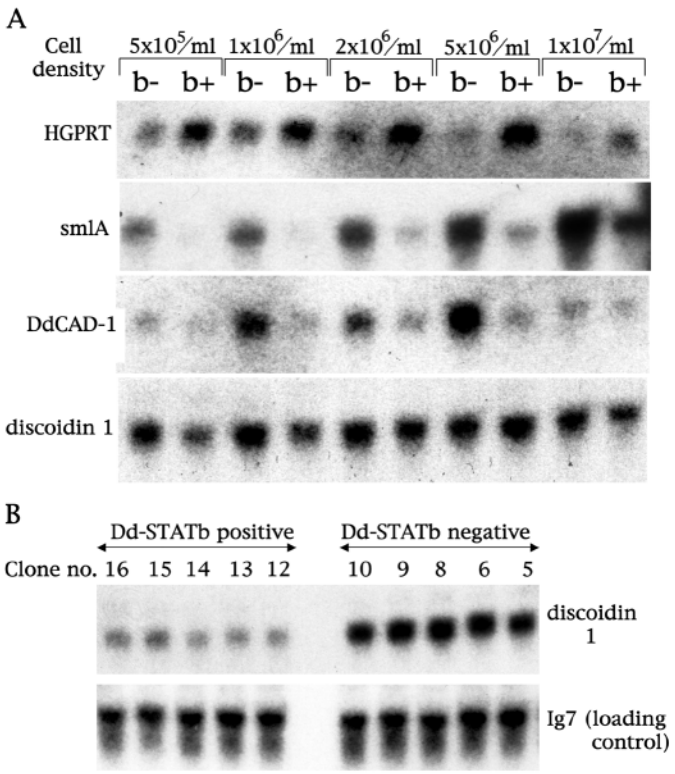

Fig. 5. (A) Confirmation of the micro-array results for four selected ESTs. In a micro-array screen of 1700 ESTs, using RNAs from growing Dd-STATb+ and Dd-STATb– cells to make the labelled cDNAs, 38 ESTs showed a reproducible difference in hybridisation (see Table 1). Several of the characterised ESTs (i.e. those where the *Dictyostelium* gene had previously been described or, in the case of HGPRT, where a function could be inferred) were employed as probes in northern transfer, using RNAs extracted from cells growing in HL5 medium and at the indicated densities. In some cases, different northern blots were used for different analyses. A loading control was performed for each blot, using the constitutively expressed gene Ig7, and in each case the control confirmed the changes visualised here (data not shown). (B) Comparison of the levels of discoidin 1 gene expression in multiple Dd-STAb+ and Dd-STATb– clone. Independent clones from the same transformation, using the Dd-STATb disruption construct, were screened for Dd-STATb expression by immunostaining. Five 'random integrant' clones (clones B12-16), where the blasticidin resistance cassette inserted non-homologously into the genome, and five Dd-STATb disruptant clones (B5, B6, B8, B9 and B10) were analysed by northern transfer using a discoidin 1 probe. The loading control shown was performed on the same blot, by melting off the discoidin 1 hybridisation signals and then using, as a probe, the constitutively expressed gene Ig7.

and 12. Thus, allowing for the relatively low resolution afforded by the gradient separation technique, the sedimentation rate of Dd-STATb is consistent with its being part of a dimer; although it could of course be monomeric Dd-STATb complexed with another protein or proteins.

Dd-STATa and Dd-STATc are the obvious candidates for other interacting proteins. Hence, we performed immunoprecipitation using the C:STATb antibody and analysed the precipitated material for the presence of Dd-STATa, Dd-STATb and Dd-STATc by western transfer (Fig. 8A). Comparison of the Dd-STAT signal obtained in the total lysate with that observed in the immunoprecipitation suggests that the recovery of Dd-STATb was approximately quantitative. Although there is a very strong signal for Dd-STATb itself, there is no trace of a signal in the migration positions of Dd-STATa or Dd-STATc. Thus, we conclude that Dd-STATb does not form a stoichometric heterodimer with Dd-STATb. A very low level of heterodimerisation might not be detected by this technique so we asked whether Dd-STATa or Dd-STATc are required for the nuclear translocation of Dd-STATb, by analysing Dd-STATb intracellular localisation in cells that are null for both Dd-STATa and Dd-STATc. Slugs obtained from the double null cells show the same punctate, nuclear staining pattern as the Ax-2 control (Fig. 8B) so we conclude that there is no obligate requirement for heterodimerisation with Dd-STATa or Dd-STATc.

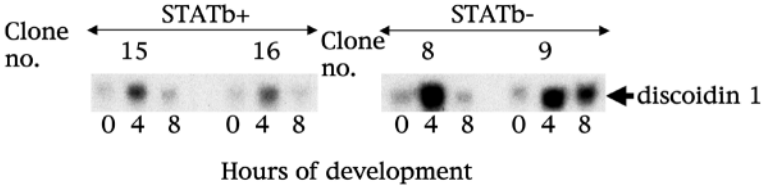

Fig. 6. Comparison of developmental changes in the levels of discoidin 1 gene expression in Dd-STAb+ and Dd-STATb– clones. The kinetics and extent of discoidin 1 mRNA accumulation were determined for two random integrant, Dd-STATb+ clones (B15 and B16, Fig. 3B) and two disruptant, Dd-STATb- clones (B8 and B9, Fig. 3B). Cells were grown to a density of 2×10^6 cells/ml and subjected to development in shaken suspension in KK2 for the indicated time periods.

Mutations within the predicted tyrosine phosphorylation site and within the SH2 domain do not impair biochemical functioning of Dd-STATb

In order to dissect the mechanism of activation of Dd-STATb further, two mutant forms of the protein were constructed and expressed in *Dictyostelium*. In the LR mutant L1025 is substituted by arginine and in the YF mutant Y1143 is substituted by phenylalanine. The LR mutation changes the SH2 domain, to more closely resemble the canonical SH2 domain (but of course the amino acid insertions remain present), while the YF mutation removes the predicted site of tyrosine phosphorylation.

The unmutated (wild type), LR and YF forms of the Dd-STATb protein were expressed under the control of a semi-constitutive promoter in Dd-STATb null cells. All three constructs produce proteins of the size expected for Dd-STATb (data not shown). We tried repeatedly to determine whether the different constructs correct the growth defect of Dd-STATb null cells, by performing co-cultivation with random integrant cells. Unfortunately, this proved impossible because of widely differing growth rates in cells overexpressing the control (i.e. the unmutated) Dd-STATb protein. The transformants were selected using G418. Hence, the integrated constructs are present at a high and variable copy number. We believe that the growth competition assay system is very sensitive to

Fig. 7. Size analysis of endogenous Dd-STATb protein on a glycerol gradient. Cells at 4 hours of development in shaken suspension were treated with 100mM sorbitol for 30 minutes (Araki et al., 2003). A whole cell protein extract was then centrifuged through a 10%-40% glycerol gradient (Fukuzawa et al., 2001). We have previously calibrated this system using commercial size markers but additionally, in this experiment, the activated (dimeric) form of Dd-STATc was generated by the sorbitol treatment and this was used as an internal marker (see text).

this variation in Dd-STATb copy number, perhaps because of a dominant-negative effect of the overexpressed Dd-STATb protein on cell growth rate.

Because we could not obtain reproducible growth results, using clones transformed with the wild-type construct, we could not study the biological behaviour of the two mutants further and this same problem also precluded the use of microarray analysis to study the Dd-STATb mutants. We therefore analysed the biochemical and cytological properties of the two mutant proteins. Both proteins sediment on glycerol gradients in the approximate position expected for a homodimer (Fig. 9) and both are nuclear enriched (Fig. 10). Hence, in so far as we are able to assay it, the two mutations do not seem to interfere with Dd-STATb function.

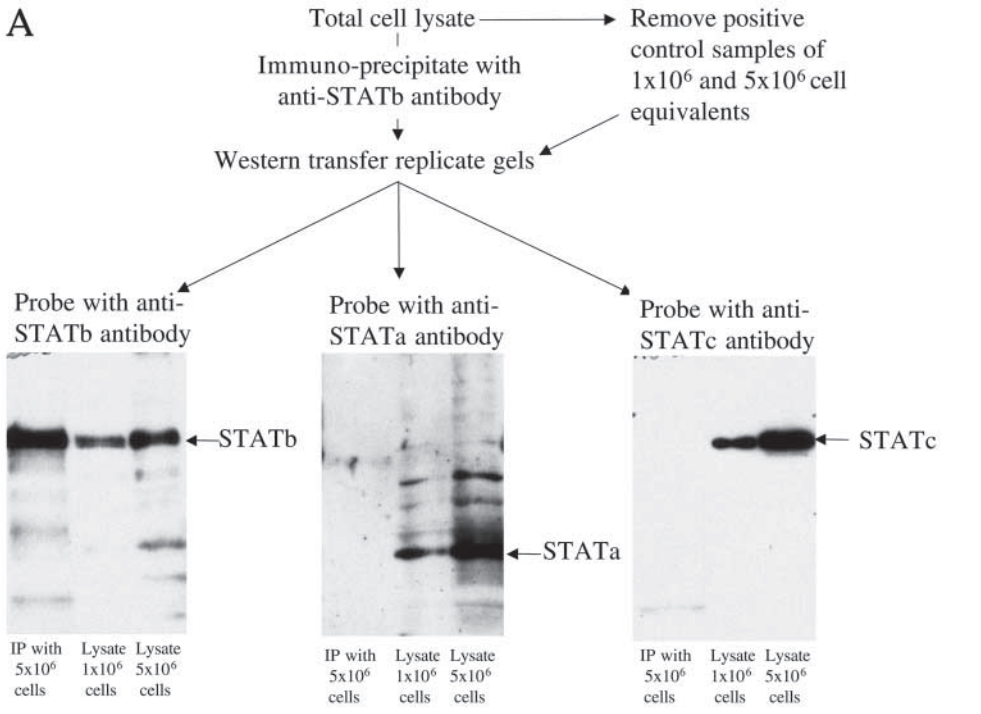

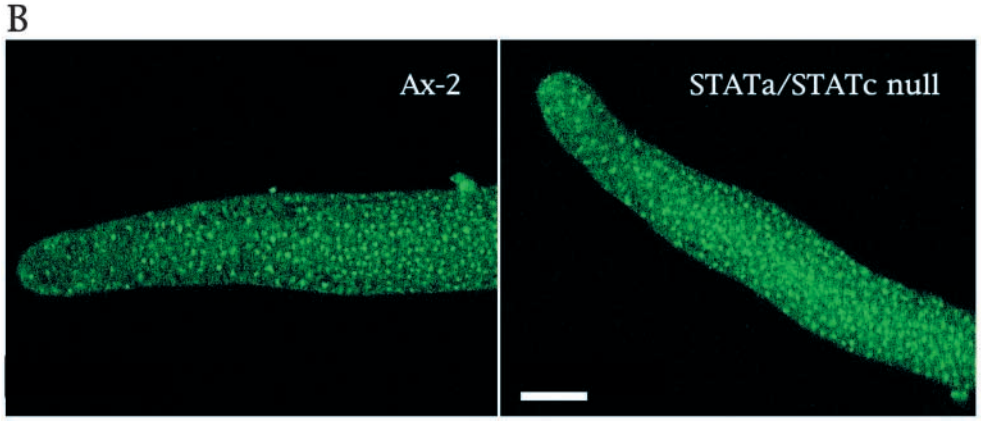

Fig. 8. Biochemical analysis of potential interactions between Dd-STATb and other STATs.
(A) Growing cells were lysed and subjected to immunoprecipitation using the C:STATb antibody and the pellet was assayed for the three STATs using the analysis protocol described on the figure. (B) Genetic analysis of potential interactions between Dd-STATb and other STATs. Slugs were generated using either Ax-2 cells or cells that are null for both the Dd-STATa and the Dd-STATc genes. The latter strain was created by sequential inactivation, using ura and blasticidin disruption cassettes (Kawata et al., 1996; Kalpaxis et al., 1991). Absence of both STAT proteins in the selected strain was confirmed immunochemically. Whole-mount slugs were fixed and stained using the C:STATb antibody and visualised by confocal microscopy. Only the front approximate half of each slug is shown and their tips are facing left.

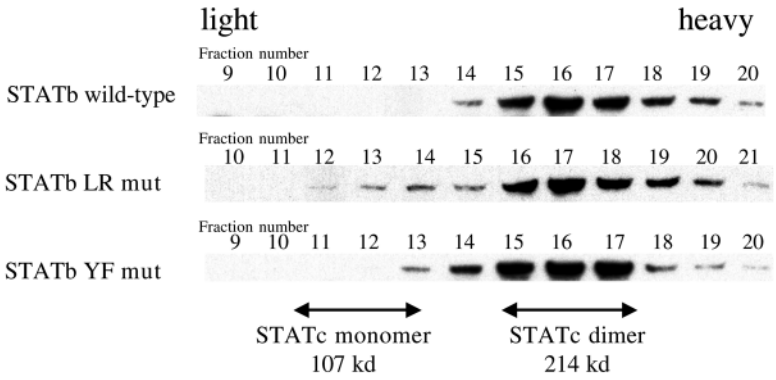

Fig. 9. Glycerol gradient analysis of unmutated and mutated forms of Dd-STATb. Two mutant versions of Dd-STATb, and the unmutated Dd-STATb, were cloned downstream of the constitutive actin 15 promoter; in LR residue L1025 is converted to arginine and in YF residue Y1143 is converted to phenylalanine. These three DNAs were stably transformed into *Dictyostelium* using G418 as the selective agent. This yields multiple copies of the transforming DNA, the number varying from cell. Clones with a high expression level were selected and analysed as described in the legend to Fig. 7. Scale bar: 10 μm.

Discussion

Dd-STATb differs from the two characterised *Dictyostelium* STATs, Dd-STATa and Dd-STATc, in a number of important respects. Both Dd-STATa and Dd-STATc become tyrosine phosphorylated and accumulate in the nucleus in a temporally and spatially constrained fashion. They achieve this specificity by responding to two different extracellular signaling molecules, cAMP and DIF. By contrast, Dd-STATb is constitutively enriched in the nuclei of all growing and developing cells. This is most easily explained by some mechanism of constitutive activation, leading to dimerisation and nuclear accumulation.

There are no apparent genetic interactions between Dd-STATb and Dd-STATa or between Dd-STATb and Dd-STATc; the double mutants display phenotypes that are indistinguishable from the Dd-STATa and Dd-STATc-null phenotypes. In addition, co-immunoprecipitation and genetic studies provide no evidence for heterodimerisation of Dd-STATb with either Dd-STATa or Dd-STATc. Our inability to detect a developmental defect in the Dd-STATb null strain, and the absence of additive effects in the Dd-STATb double mutants with Dd-STATa and c, led us to employ a growth competition assay to search for a role for Dd-STATb. This revealed a phenotype; Dd-STATb null (Dd-STATb–) cells are at a growth disadvantage when subjected to multiple cycles of co-cultivation with Dd-STATb+ cells.

The weak growth phenotype led us to perform micro-array analysis using RNA from growing Dd-STATb+ and Dd-STATb– cells. Twenty-nine genes, from the total of 1700 non-redundant ESTs analysed, were overexpressed in Dd-STATb null cells while nine genes were underexpressed. There is a clear preponderance of overexpressed genes and, in this context, all three *Dictyostelium* STATs share one interesting characteristic; they lack the C-terminal transactivation domains that are a general feature of metazoan STATs. This may explain why Dd-STATa and Dd-STATC also serve as transcriptional repressors (Mohanty et al., 1999; Fukuzawa et al., 2001).

The microarray results were confirmed for HGPRT, a gene that is underexpressed in the null strain, and for three of the genes that are overexpressed: smlA, discoidin 1 and Dd-CAD-1. The SmlA protein controls the secretion of a factor that regulates the number of cells that participate in the formation of individual developing structures (Brock et al., 1996). We see no effect on territory size because of the overexpression of smlA but, in the microarray assay, we surveyed only about 15% of the expressed genes in the organism and any number of other changes could be occurring to ameliorate the effects of the quantitative change in SmlA levels. Dd-CAD-1 is a Ca^{2+}-dependent cell adhesion molecule (Wong et al., 1996). Interestingly, growth conditions have a significant effect on the expression of Dd-CAD-1 (Yang et al., 1997). In addition, the three discoidin I genes are particularly well characterised as markers of the growth-development transition (under the hybridisation conditions used, the probe probably recognises the transcripts of all three discoidin 1 genes, so we will assume we are analysing their composite behaviour).

Discoidins Iα, Iβ and Iγ encode developmentally regulated lectins. The three genes are not expressed

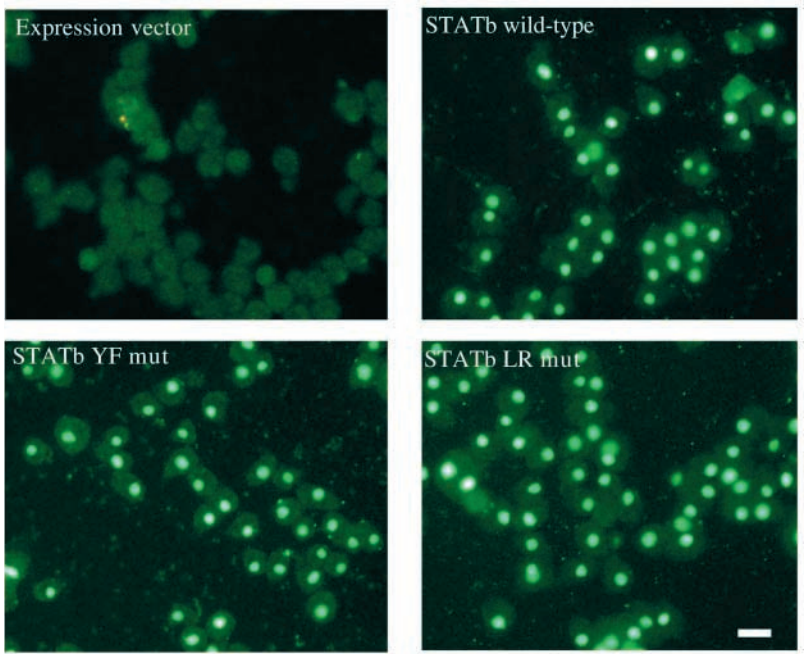

Fig. 10. Immunohistochemical analysis of cells expressing unmutated and mutated forms of Dd-STATb. Growing cells expressing the unmutated and mutated versions of Dd-STATb, described in Fig. 8 were subjected to immunohistochemical analysis exactly as described in Fig. 3. Scale bar: 100 μm.

in bacterially grown cultures at low cell densities but cells growing in axenic culture express the discoidin Iα and Iγ genes at a low level (Devine et al., 1982). Two different protein factors, PSF and CMF, serve as cell density sensors, regulating discoidin gene expression (Rathi et al., 1991; Blusch et al., 1995) and the signalling pathway has been extensively characterised; PKA, RasG and Gα2 all function as modulators of discoidin I gene expression (Primpke et al., 2000; Secko et al., 2001; Blusch et al., 1995), and the promoter of the discoidin Iγ gene has been dissected into its functional components (Vauti et al., 1990). It will be of interest to determine how Dd-STATb fits into this complex regulatory network.

The above studies show that Dd-STATb is nuclear enriched, that it regulates gene expression, both during growth and development, and that it is required for optimal cell growth. The fact that Dd-STATb is a cellular regulator was not, however, at all predictable from its structure. Dd-STATb contains a DNA-binding domain and a site of tyrosine phosphorylation that are well conserved relative to metazoan STATs but the SH2 domain displays two highly unusual features that might have been expected to abrogate its function: a 15 amino acid insertion and the substitution of an otherwise invariant arginine residue.

In the absence of a three-dimensional structure for Dd-STATb, it is difficult to judge the extent of the functional disruption caused by the structural variation and therefore a modelling study was carried out. The substituted arginine residue (R175 in pp60$^{c\text{-}src}$) is universally conserved among SH2 domains, it makes direct ionic interactions with the phosphate group of the phosphotyrosine and is the residue that is usually subjected to site-specific mutation when an SH2 domain is to be inactivated (Bibbins et al., 1993; Bradshaw et al., 1999; Shuai et al., 1993; Tian and Martin, 1996). Indeed, the equivalent arginine residue fulfils the same function, of binding phosphotyrosine, in the most divergent SH2 domain described to date; that of the Cbl oncogene, a highly abnormal SH2 domain that was only clearly recognised as such when its three dimensional structure was determined (Meng et al., 1999).

The presence of such an unusual SH2 domain in Dd-STATb is intriguing, because SH2 domains were discovered in the metazoa and *Dictyostelium* is the only non-metazoan species shown to possess functional SH2 domains. The SH2 domain of Dd-STATb could, therefore, be providing an insight into ancestral SH2 domains; lost during animal evolution but retained in *Dictyostelium*. However, it is equally possible that the form of SH2 domain found in Dd-STATb arose after the divergence of metazoa and protozoa and that it affords *Dictyostelium* a signalling potential not possessed by animals.

There are metazoan precedents that may provide insights into the mode of action of the Dd-STATb SH2 domain. The fact that STAT1 and STAT3 homodimerise prior to their activation (Braunstein et al., 2003) indicates that STAT proteins have an intrinsic capacity for self association. However, the STAT homodimers so formed do not bind to DNA (Braunstein et al., 2003), hence they are biologically non-functional. By contrast, the SH2 domain of SAP, the product of the gene mutated in X-linked lymphoproliferative syndrome, functions by binding to a specific sequence within the cytoplasmic tail of the SLAM (Coffey et al., 1998; Nichols et al., 1998; Sayos et al., 1998). Structural and biochemical analysis shows that the recognition site within SLAM is bound by the phosphotyrosine binding pocket of SAP in a mode that does not require tyrosine phosphorylation (Poy et al., 1999; Sayos et al., 1998). This interaction is possible because the SAP binding site, within the SLAM receptor, contains additional residues, upstream of the site of tyrosine phosphorylation, that are not present in orthodox SH2 domain-binding sites and that are specifically recognised by the SAP SH2 domain.

The above example shows how an SH2 domain can functionally interact with a non-tyrosine phosphorylated ligand but SLAP is a highly unorthodox, ‘free’ SH2 domain protein; as its name implies it is comprised of only an SH2 domain with a very small C-terminal extension. However, there is a prior study with an R to L mutant form of an SH2 domain within the context of a larger protein. When R175 within the Src SH2 domain is mutated to leucine, binding to a Src phosphopeptide is almost completely eliminated (Bibbins et al., 1993). Surprisingly, binding to a peptide from the PDGF receptor (PD751) is only marginally reduced. Furthermore, binding of the R to L mutant SH2 domain to the PDGF receptor peptide occurs via a mechanism that is again independent of tyrosine phosphorylation.

The fact that SH2 domains can, under some circumstances, interact with non-tyrosine phosphorylated ligands is of course relevant only if Dd-STATb is not tyrosine phosphorylated in vivo. Limited support for this idea comes from our inability to detect tyrosine phosphorylation of Dd-STATb, using an antibody specific for phosphotyrosine to probe immunoprecipitated Dd-STATb protein (N.V.Z. and J.G.W., unpublished). This result should not, however, be over-interpreted, because a very low level of tyrosine phosphorylation may not have been detected but could be biologically significant. A much more telling result derives from mutational analysis. The Y to F mutant of Dd-STATb functions sediments as a dimer and is nuclear enriched. In combination, these facts suggest that Dd-STATb functions by a mechanism that is significantly different from the standard STAT paradigm.

This work was supported by Wellcome Trust Program Grant 039899/Z to J.G.W. and would not have been possible without the kind gift of the ESTs by the Japanese cDNA consortium.

References

Araki, T., Gamper, M., Early, A., Fukuzawa, M., Abe, T., Kawata, T., Kim, E., Firtel, R. A. and Williams, J. G. (1998). Developmentally and spatially regulated activation of a *Dictyostelium* STAT protein by a serpentine receptor. *EMBO J.* **17**, 4018-4028.

Araki, T., Tsujioka, M., Abe, T., Fukuzawa, M., Meima, M., Schaap, P., Morio, T., Urushihara, H., Katoh, M., Maeda, M. et al. (2003). A STAT-regulated, stress-induced signalling pathway in *Dictyostelium*. *J. Cell Sci.* **116**, 2907-2915.

Bibbins, K. B., Boeuf, H. and Varmus, H. E. (1993). Binding of the Src SH2 domain to phosphopeptides is determined by residues in both the SH2 domain and the phosphopeptides. *Mol. Cell Biol.* **13**, 7278-7287.

Blusch, J., Alexander, S. and Nellen, W. (1995). Multiple signal transduction pathways regulate discoidin I gene expression in *Dictyostelium*. *Differentiation* **58**, 253-260.

Bradshaw, J. M., Mitaxov, V. and Waksman, G. (1999). Investigation of phosphotyrosine recognition by the SH2 domain of the Src kinase. *J. Mol. Biol.* **293**, 971-985.

Brock, D. A., Buczynski, G., Spann, T. P., Wood, S. A., Cardelli, J. and

Gomer, R. H. (1996). A *Dictyostelium* mutant with defective aggregate size determination. *Development* **122**, 2569-2578.
Braunstein, J., Brutsaert, S., Olson, R. and Schindler, C. (2003). STATs Dimerize in the absence of phosphorylation. *J. Biol. Chem.* **278**, 34133-34140.
Bromberg, J. and Darnell, J. E., Jr (2000). The role of STATs in transcriptional control and their impact on cellular function. *Oncogene* **19**, 2468-2473.
Chatterjee-Kishore, M., van den Akker, F. and Stark, G. R. (2000). Association of STATs with relatives and friends. *Trends Cell Biol.* **10**, 106-111.
Chen, X., Vinkemeier, U., Zhao, Y., Jeruzalmi, D., Darnell, J. E., Jr and Kuriyan, J. (1998). Crystal structure of a tyrosine phosphorylated STAT-1 dimer bound to DNA. *Cell* **93**, 827-839.
Coffey, A. J., Brooksbank, R. A., Brandau, O., Oohashi, T., Howell, G. R., Bye, J. M., Cahn, A. P., Durham, J., Heath, P., Wray, P. et al. (1998). Host response to EBV infection in X-linked lymphoproliferative disease results from mutations in an SH2-domain encoding gene. *Nat. Genet.* **20**, 129-135.
Devine, J. M., Tsang, A. S. and Williams, J. G. (1982). Differential expression of the members of the discoidin I multigene family during growth and development of *Dictyostelium*. *Cell* **28**, 793-800.
Fukuzawa, M. and Williams, J. G. (2000). Analysis of the promoter of the cudA gene reveals novel mechanisms of *Dictyostelium* cell type differentiation. *Development* **127**, 2705-2713.
Fukuzawa, M., Hopper, N. A. and Williams, J. G. (1997). *cudA*: a *Dictyostelium* gene with pleiotropic effects on cellular differentiation and slug behaviour. *Development* **124**, 2719-2728.
Fukuzawa, M., Araki, T., Adrian, I. and Williams, J. G. (2001). Tyrosine phosphorylation-independent nuclear translocation of a *Dictyostelium* STAT in response to DIF signaling. *Mol. Cell* **7**, 779-788.
Horvath, C. M. (2000). STAT proteins and transcriptional responses to extracellular signals. *Trends Biochem. Sci.* **25**, 496-502.
Kalpaxis, D., Zundorf, I., Werner, H., Reindl, N., Boy-Marcotte, E., Jacquet, M. and Dingermann, T. (1991). Positive selection for Dictyostelium discoideum mutants lacking UMP synthase activity based on resistance to 5-fluoroorotic acid. *Mol. Gen. Genet.* **225**, 492-500.
Kawata, T., Shevchenko, A., Fukuzawa, M., Jermyn, K. A., Totty, N. F., Zhukovskaya, N. V., Sterling, A. E., Mann, M. and Williams, J. G. (1997). SH2 signaling in a lower eukaryote: A STAT protein that regulates stalk cell differentiation in *Dictyostelium*. *Cell* **89**, 909-916.
Meng, W., Sawasdikosol, S., Burakoff, S. J. and Eck, M. J. (1999). Structure of the amino-terminal domain of Cbl complexed to its binding site on ZAP-70 kinase. *Nature* **398**, 84-90.
Mohanty, S., Jermyn, K. A., Early, A., Kawata, T., Aubry, L., Ceccarelli, A., Schaap, P., Williams, J. G. and Firtel, R. A. (1999). Evidence that the *Dictyostelium* Dd-STATa protein is a repressor that regulates commitment to stalk cell differentiation and is also required for efficient chemotaxis. *Development* **126**, 3391-3405.
Moniakis, J., Funamoto, S., Fukuzawa, M., Meisenhelder, J., Araki, T., Abe, T., Meili, R., Hunter, T., Williams, J. and Firtel, R. A. (2001). An SH2-domain-containing kinase negatively regulates the phosphatidylinositol-3 kinase pathway. *Genes Dev.* **15**, 687-698.
Morio, T., Urushihara, H., Saito, T., Ugawa, Y., Mizuno, H., Yoshida, M., Yoshino, R., Mitra, B. N., Pi, M., Sato, T. et al. (1998). The *Dictyostelium* developmental cDNA project: generation and analysis of expressed sequence tags from the first-finger stage of development. *DNA Res.* **5**, 335-340.
Nichols, K. E., Harkin, D. P., Levitz, S., Krainer, M., Kolquist, K. A., Genovese, C., Bernard, A., Ferguson, M., Zuo, L., Snyder, E. et al. (1998). Inactivating mutations in an SH2 domain-encoding gene in X-linked lymphoproliferative syndrome. *Proc. Natl. Acad. Sci. USA* **95**, 13765-13770.
Pawson, T., Gish, G. D. and Nash, P. (2001). SH2 domains, interaction modules and cellular wiring. *Trends Cell Biol.* **11**, 504-511.
Ponte, E., Bracco, E., Faix, J. and Bozzaro, S. (1998). Detection of subtle phenotypes: The case of the cell adhesion molecule csA in Dictyostelium. *Proc. Natl. Acad. Sci. USA* **95**, 9360-9365.
Ponte, E., Rivero, F., Fechheimer, M., Noegel, A. and Bozzaro, S. (2000). Severe developmental defects in Dictyostelium null mutants for actin-binding proteins. *Mech. Dev.* **91**, 153-161.
Poy, F., Yaffe, M. B., Sayos, J., Saxena, K., Morra, M., Sumegi, J., Cantley, L. C., Terhorst, C. and Eck, M. J. (1999). Crystal structures of the XLP protein SAP reveal a class of SH2 domains with extended, phosphotyrosine-independent sequence recognition. *Mol. Cell* **4**, 555-561.
Primpke, G., Iassonidou, V., Nellen, W. and Wetterauer, B. (2000). Role of cAMP-dependent protein kinase during growth and early development of *Dictyostelium*. *Dev. Biol.* **221**, 101-111.
Rathi, A., Kayman, S. C. and Clarke, M. (1991). Induction of gene expression in *Dictyostelium* by prestarvation factor, a factor secreted by growing cells. *Dev. Genet.* **12**, 82-87.
Sayos, J., Wu, C., Morra, M., Wang, N., Zhang, X., Allen, D., van Schaik, S., Notarangelo, L., Geha, R., Roncarolo, M. G. et al. (1998). The X-linked lymphoproliferative-disease gene product SAP regulates signals induced through the co-receptor SLAM. *Nature* **395**, 462-469.
Secko, D. M., Khosla, M., Gaudet, P., Tsang, A., Spiegelman, G. B. and Weeks, G. (2001). RasG regulates discoidin gene expression during *Dictyostelium* growth. *Exp. Cell Res.* **266**, 135-141.
Shuai, K., Ziemiecki, A., Wilks, A. F., Harpur, A. G., Sadowski, H. B., Gilman, M. Z. and Darnell, J. E. (1993). Polypeptide signalling to the nucleus through tyrosine phosphorylation of Jak and Stat proteins. *Nature* **366**, 580-583.
Shuai, K., Horvath, C. M., Huang, L. H., Qureshi, S. A., Cowburn, D. and Darnell, J. E., Jr (1994). Interferon activation of the transcription factor Stat91 involves dimerization through SH2-phosphotyrosyl peptide interactions. *Cell* **76**, 821-828.
Summers, N. L. and Karplus, M. (1989). Construction of side-chains in homology modelling. Application to the C-terminal lobe of rhizopuspepsin. *J. Mol. Biol.* **210**, 785-811.
Tian, M. and Martin, G. S. (1996). Reduced phosphotyrosine binding by the v-Src SH2 domain is compatible with wild-type transformation. *Oncogene* **12**, 727-734.
Vauti, F., Morandini, P., Blusch, J., Sachse, A. and Nellen, W. (1990). Regulation of the discoidin-Igamma-gene in *Dictyostelium* – identification of individual promoter elements mediating induction of transcription and repression by cyclic AMP. *Mol. Cell. Biol.* **10**, 4080-4088.
Watts, D. J. and Ashworth, J. M. (1970). Growth of myxamoebae of the cellular slime mould *Dictyostelium* in axenic culture. *Biochem. J.* **119**, 171-174.
Wong, E. F. S., Brar, S. K., Sesaki, H., Yang, C. Z. and Siu, C. H. (1996). Molecular cloning and characterization of DdCAD-1, a Ca2+-dependent cell-cell adhesion molecule, in *Dictyostelium*. *J. Biol. Chem.* **271**, 16399-16408.
Yang, C. Z., Brar, S. K., Desbarats, L. and Siu, C. H. (1997). Synthesis of the Ca2+-dependent cell adhesion molecule DdCAD-1 is regulated by multiple factors during *Dictyostelium* development. *Differentiation* **61**, 275-284.